

Azo Dye Decolorization in Bioelectrochemical System: Characteristic Analysis of Electrochemical Active Biofilms

You-Zhao Wang^{1,*}, Ai-juan Zhou², Yuan-Hua Xie¹, Jin Han¹, Mei-Yan You¹, Min Wang¹, Tong Zhu^{1,*}

¹ Institute of Process Equipment and Environmental Engineering, School of Mechanical Engineering and Automation, Northeastern University, Shenyang 110004, PR China

² College of Environmental Science and Engineering, Taiyuan University of Technology, Taiyuan 030024, PR China

*E-mail: wangyz@me.neu.edu.cn, tongzhu@mail.neu.edu.cn

Received: 15 May 2016 / Accepted: 30 June 2016 / Published: 7 August 2016

Electrochemical active biofilms (EABs) have attracted considerable attractions in bioelectrochemical systems (BESs) field for pollutants degradation from waste water. However, few studies have looked at EABs formation influenced by anode and cathode conditions. Therefore, EABs feature was investigated under different electrode conditions using a single-chamber BES. After EABs formation, the BES was effective in decolorizing the targeted pollutant azo dye, comparing to abio-electrode BESs. By analyzing the EABs microbial community compositions, anode EAB was dominated by a model electro-active *Geobacter* (29%), whereas the cathode EAB microbial structure was relatively closer to the inoculum with low abundance *Geobacter* (2.5%). This study suggested that changing the inoculum composition would be conducive to improving the cathode EAB capability for recalcitrant pollutant degradation in actual engineering applications.

Keywords: bioelectrochemical system; electrochemical active biofilm; azo dye; decolorization

1. INTRODUCTION

The bioelectrochemical system is developing rapidly and being applied to solve environmental issues, including energy generation and recalcitrant pollutants removal[1]. According to different electron acceptors, the oxygen is reduced to generate electric energy (microbial fuel cells, MFCs)[2, 3], or the proton is reduced to H₂ (microbial electrolysis cells, MECs)[4], until some pollution can also be reduced in recent years, such as azo dye, chloric compounds, nitrate, and heavy metal, *etc.*[5-8] Comparing to conventional anaerobic digestion and electrochemical technology, higher reaction

efficiency, low power consumption and environmental sustainability will drive BESs to attract more attention in wastewater treatment field.

In BESs, electrochemical active biofilms (EABs) existing on anode (bioanode) oxidize substrate to release electrons by direct or indirect extracellular electron transfer (EET) [9, 10], and then these electrons pass the external circuit to cathode, where some noble metal as catalyst (such as platinum) accelerate the cathodic reduction rate (abio-cathode). An alternative for cathode catalyst is necessary because noble metal catalyst is expensive, non-renewable and catalyst poisoning. Furthermore, EABs as cathodic catalysts (biocathode) also become another hot topic in BESs field due to low cost, environmental sustainability and its ability to enhance the cathode reduction with better BES performance[11, 12]. Up to now, biocathode has been developed into a wider application range, such as biosynthesis of organic matter [13], based on the multifunctional EABs[14].

Of course, considerable studies about EABs have focused on the various functions or EET mechanisms due to its great potential [15, 16]. However, there are few reports on how the different electrode conditions influence the EABs formation, which is important for further practical engineering, considering EABs simultaneous formation (bioanode and biocathode) in single-chamber BESs without ion exchange membrane separation. Besides, many studies showed that the EABs of anode and cathode were constructed in the two-chamber BES using two different inoculums to achieve the better performance, but only one inoculum usually can be chosen for both EABs formation in the single-chamber BES during BES startup. The different electrode conditions will influence the EAB community structure that finally decide the performance of BES. It is necessary that understanding the characteristics of both EABs.

Azo dye as common pollutants in dyeing waste water can be decolorized by BESs cathode since the electrons from anode can break the chromogenic azo bonds of azo dye. This study investigated the EAB formation in BES anode and cathode, based on same inoculum. Then the azo dye was as the targeted pollutant to evaluate EABs degradation performance and finally EABs community structures were analyzed for further understanding the EABs formation characteristics.

2. MATERIALS AND METHODS

2.1 BES set-up and bio-electrode analysis

All experiments were conducted at room temperature (23~25°C). The membrane-less, single-chamber BES was constructed by plexiglas and its shape was cuboid with a cylindrical cavity (140 ml in internal volume). Both anode and cathode were carbon brush (ID 4.5 cm * L 4.0 cm), saturated calomel electrode (SCE, +0.241 V vs. standard hydrogen electrode, Shanghai Precision Scientific Instruments Co. Ltd, China) was a reference electrode to measure the electrode potentials. Anode and cathode were connected by direct current power supply. A precise resistor (10 Ω) with the power supply in series was connected in the circuit. The data acquisition (Keithley 2700, Keithley Co., Ltd., USA) was connected all electrodes and resistor for collecting the voltage signal, including the potentials of anode and cathode, and the voltage of resistor. The current of BES was measured through the resistor voltage based on the Ohm's law. The reaction solution contained (g L⁻¹): acetate, 0.82;

NaH₂PO₄·2H₂O, 2.77; Na₂HPO₄·12H₂O, 11.55; NH₄Cl, 0.31; KCl, 0.13. The inoculum of this setup was enriched from effluent of BES used for azo dye waste water treatment in previous study [17]. Electrochemical impedance spectroscopy (EIS) was performed to characterize the charge transfer resistance (R_{ct}) of working electrode ($10^5 \sim 10^2$ Hz, 5 mV sine wave) using electrochemical workstation (model-660D, CH Instruments Inc., USA), and the obtained data was simulated by ZsimpWin3.10 software using R (QR) equivalent equation.

2.2 Analysis of azo dye decolorization

After bio-electrode formation, the single-chamber BES was operated in batch mode with 12 h as test cycle. The amido black 10B as targeted azo dye was injected to reaction solution when test cycle began. The amido black 10B concentration was measured by spectrophotometry and its maximum absorption wavelength is 618 nm. The azo dye decolorization efficiency (DE), electrons recovery efficiency for azo dye (ERE), and specific energy consumption (SEC) were calculated as follows:

$$DE = \frac{C_0 - C_t}{C_0} \times 100\% \quad (1)$$

$$ERE = \frac{14F(C_0 - C_t)V}{M_{azo} \int_0^t I dt} \times 100\% \quad (2)$$

$$SEC = \frac{U \int_0^t I dt}{(C_0 - C_t)V} \quad (3)$$

Where C_0 and C_t represents the initial concentration and test cycle end concentration of azo dye, g L⁻¹; I, reactor current(A); F, Faraday's constant (96485 C mol⁻¹e⁻¹); V, the reactor volume (0.14 L); M_{azo} , amido black 10B molecular weight (616.49 g mol⁻¹); U, supply power voltage (V).

The azo dye decolorization was fitted using apparent first-order reaction model with equation. The K represents the rate constant calculated by software ORIGIN 8.0:

$$C_t = C_0 e^{-kt} \quad (4)$$

2.3 DNA extraction and pyrosequencing

After EABs formation, the DNA samples (including inoculum) were extracted. The carbon fibers were cut from electrodes and then put in PBSs by oscillation for 10 minutes. Removing the fibers, the PBSs including bacteria was 10000 g centrifuged in 10 minutes. The pellets were for DNA extraction using a PowerSoil DNA Isolation Kit (MoBio Laboratories, Inc., Carlsbad, CA), according to the manufacturer's direction. The bacterial primers 8F (5'-AGAGTTTGATCCTGGCTC AG-3') and 533R (5'-TTACCGCGGCTGCTGGCAC-3') were to amplify the V1-V3 tags of 16S rDNA. The purified, quantified PCR products were used for 454 pyrosequencing according standard process.

2.4 Sequences data analysis

Following pyrosequencing, the primer sequences were cut out and then removed the shorter length (<200 bp) sequences and low-quality sequences[18]. The final sequences data were clustered to operational taxonomic units (OTUs) by furthest neighbor a 97% similarity (<http://www.mothur.org/wiki/Cluster>). MOTHUR software was used to evaluate the community richness index (Chao1, ACE), Community Diversity Index (Shannon, Simpson) and Good’s Coverage Index. Besides, Principal Component Analysis (PCA) was also conducted by MOTHUR. Based on the sequences data, the samples communities were affiliated to phylum, class and genus level.

3. RESULTS AND DISCUSSION

3.1 Simultaneous EABs formation

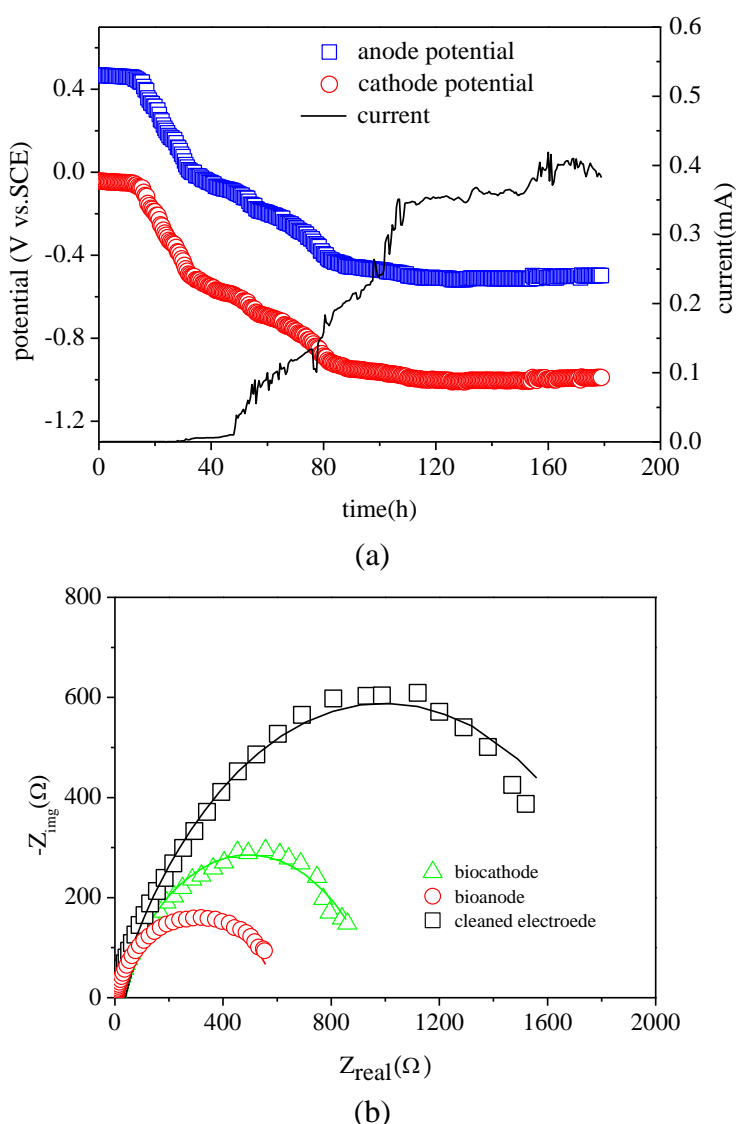


Figure 1. Analysis of EAB formation after inoculation in BES (a) Evolution of the potentials and current (b) EIS tests

After inoculation, the data recorder was performed for collecting the data of electrode potentials and current under 0.5V power supply (Fig.1A). In the initial stage, the observation of current production retained a low magnitude due to the high electrode potentials: initial potentials of anode and cathode were 0.46 V and -0.05 V, respectively. Not many electrons were released to the external circuit from substrate by anode oxidation and the electrons reduction rate finally depend on the terminal electron acceptor in which only protons existing in reaction solution which require a lower cathode potential below -0.414 V (vs. SHE, pH=7, 298 K), during EABs formation process without azo dye addition. Along with the extension of time, the potentials were decreasing gradually and stabilized around -0.5 V of anode and -1.0 V of cathode. The anode potential was very close to the theoretical potential of acetate oxidation (-0.54 V vs. SCE) that indicated the EAB formed on anode surface. Correspondingly, the current evolution had a significant increasing that also proved the bioanode formation with an ability of electrons generation.

However, it was difficult to predict the cathode EAB formation from the perspective of cathode potential. In order to better understand, the EIS was performed to analyze the electrode resistance, as shown in FIG.1B. Look at the semicircles which correspond with electrode R_{ct} , an obvious change was obtained on day 7 .By simulating the obtained data, the cathodic R_{ct} was reduced to 986 Ω less than 1989 Ω of cleaned electrode, indicating that the cathode EAB formation enriched from inoculum, because the microbes of inoculum could enhance the electron transfer from electrode to electron acceptor, it then resulted in R_{ct} evolution of electrode. In addition to cathode EAB, the anode EAB formation was also confirmed by EIS. The above results indicated that both EABs constituted the bio-electrodes and the BES startup was successful.

In two-chamber BES, as anodic EAB inoculum, the aerobic or anaerobic sludge is a good choice attributed to the high biomass and many studies used it to construct the anode EAB; as the cathodic inoculum, the targeted pollutants reducing consortium was usually used to improve the cathodic performance. In contrast, the single-chamber BES only can choose one inoculum to construct the two EABs. The previous study demonstrated that the cathodic EAB could spontaneously form using the planktonic microbes from anode EAB as inoculum[19], but it spend a lot time duo to the low concentration of planktonic biomass. Here we enriched a high concentration inoculum and simultaneously constructed the EABs of anode and cathode that accelerated the BES start-up process and be conducive to BES scale-up. However, both EABs needs not only to analyze by electrochemical monitoring, but also need to further investigation on its performance, especially to the cathode EAB, which might catalyze the reductive degradation of pollutants.

3.2 Azo dye decolorization under different power supply

After EABs formation, azo dye amido black 10B was injected to the BES as targeted pollutant with initial concentration of 100 mg L⁻¹. In order to comprehensively evaluate the BES performance, various power supply voltage were considered due to it effectively drive the azo dye decolorization with open circuit cycle as control test[20].

As shown in Fig.2a, the average potential of anode stably maintained at about -400 mV under various power voltage, little more than the -500 mV in BES startup due to the reaction solution

replacement, which could shock the anode EABs when beginning test cycle. The cathode potential increased linearly from -900 mV to -400 mV in response to power supply voltage from 500 mV to 0 mV. The increased cathode potential could reduce the electron reduction rate and resulted in a significantly decreased current.

Affected by the changed current, azo dye decolorization was enhanced by 0.5 V power supply with a maximum decolorization efficiency of 91%. With power supply voltage decreased to 0.3 V and 0.1 V, the average decolorization efficiencies were 78.2% and 50.4%, respectively (Fig.2b). A conventional decolorization process was found: the decolorization efficiency of 43.9% was obtained at open circuit mode (without power supply), since azo dye could be decolorized by microbes under anaerobic conditions, no cathodic reductive decolorization was involved in this process (FIG.3). Based on azo dye decolorization efficiency and test cycle time, the azo dye removal rate also changed with the different power supply voltage.

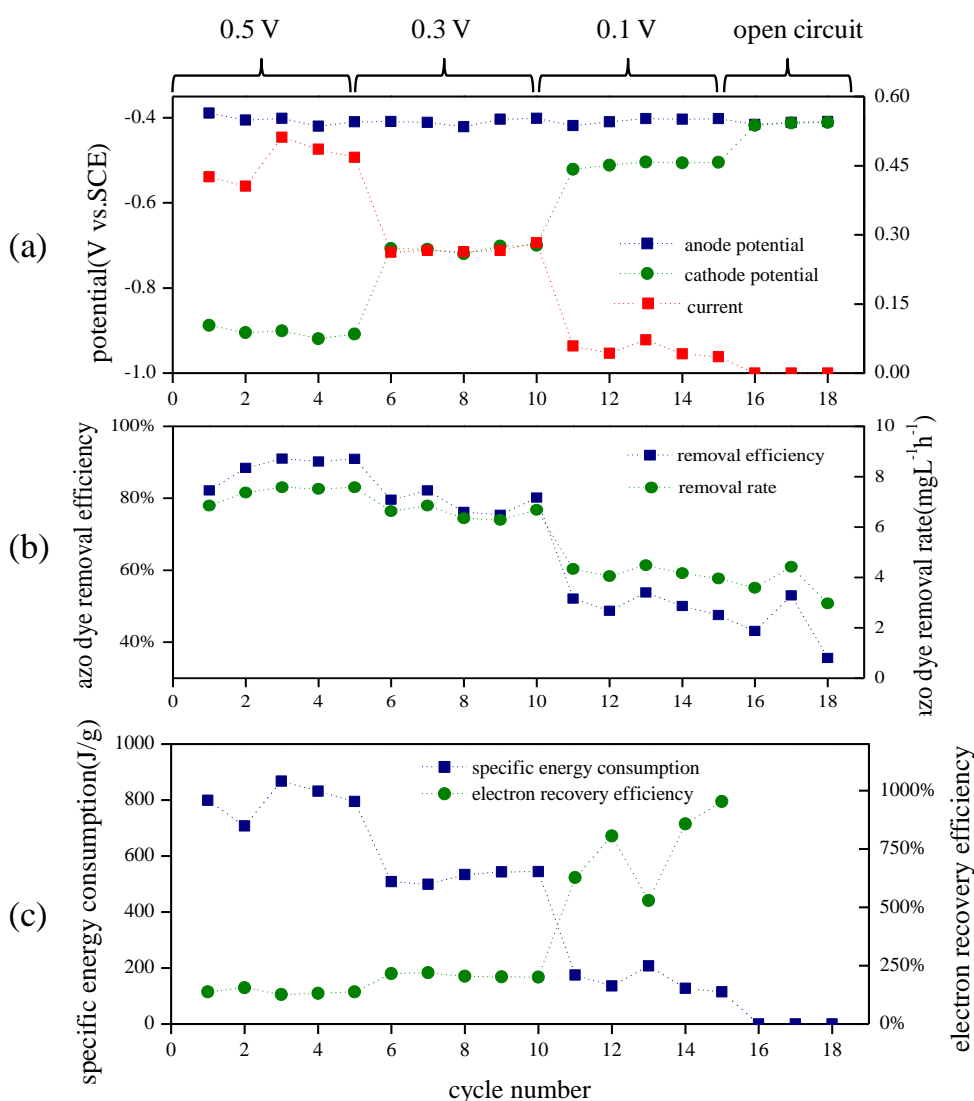


Figure 2. Analysis of azo dye decolorization under different power supply (a) change of electrode potentials and current; (b) removal efficiency and rate of azo dye (c) change of SEC and ERE

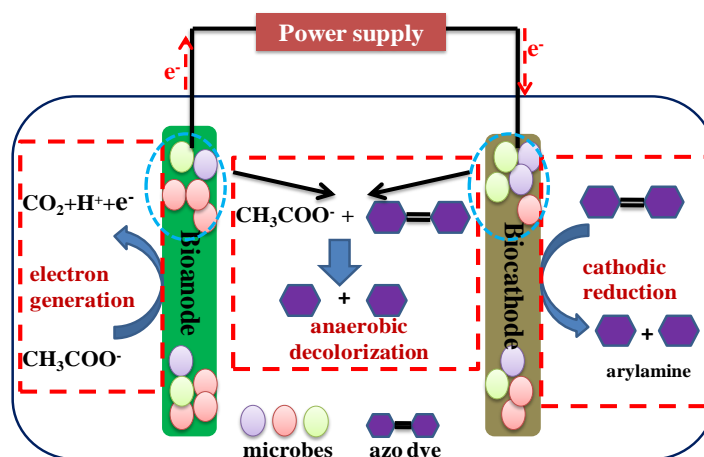


Figure 3. Schematic diagram of azo dye decolorization in single-chamber BES

As seen Fig.2c, although the higher power supply could accelerate the azo dye decolorization, the specific energy consumption (SEC) for each gram of azo removal was notably increased to 800 J g^{-1} at 0.5 V power supply, which was 1.71 and 5.26 times higher than 0.3 V and 0.1 V power supply, respectively. In contrast, the open circuit mode does not need the electrical energy, but the low azo dye decolorization rate was obtained by comparing it to power supply test. The electron recovery efficiency (ERE) could explain the excessive SEC at higher power supply voltage. The ERE was gradually decreased from 103.6% at 0.5 V power supply to 70.6% at 0.1 V power supply. Generally, the ERE could not exceed 100% in response to that all the electrons from bioanode generation were involved in cathodic reduction of azo dye. But, the partial azo dye here was decolorized by anaerobic microbes without consuming the electrons from bioanode, resulting in the ERE over 100% in the single-chamber BES (Fig.3). However, the relatively lower ERE at high power supply voltage suggested that part of these electrons might be accepted by cathodic microbes as energy resource to support its metabolism, were not involved in cathodic reduction of azo dye. These results indicated that the additional electric energy input was cost by cathode EAB for accelerating the azo dye decolorization rate.

3.3 Effect of EABs in BES

Instead of chemical catalysts, EABs as alternative catalyst also could enhance the electron transfer, especially in biocathode where the azo dye could be decolorized. In order to evaluate the feasibility of simultaneous EABs formation strategy, further analysis was performed that using same clear electrodes as abio-electrode to replace the bio-electrodes. The control groups including bioanode+abio-cathode (BA), abioanode+biocathode (AB) and abioanode+abio-cathode (AA), were set up, comparing to the targeted experimental group bioanode+biocathode (BB).The result shown in Figure 4.

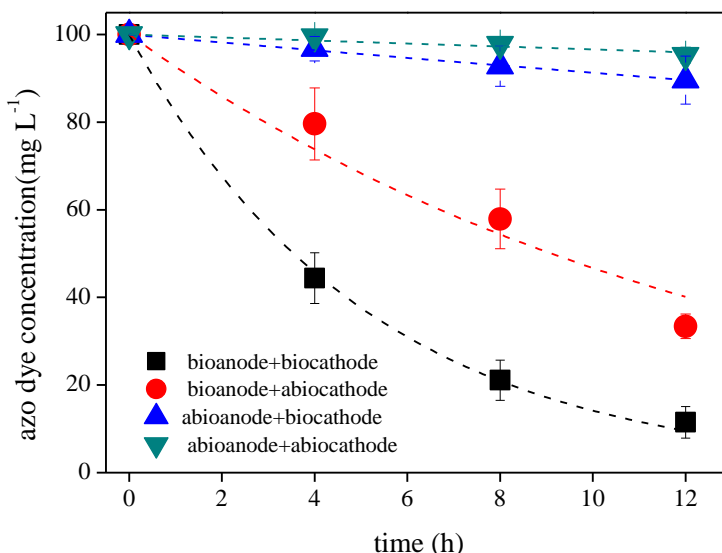
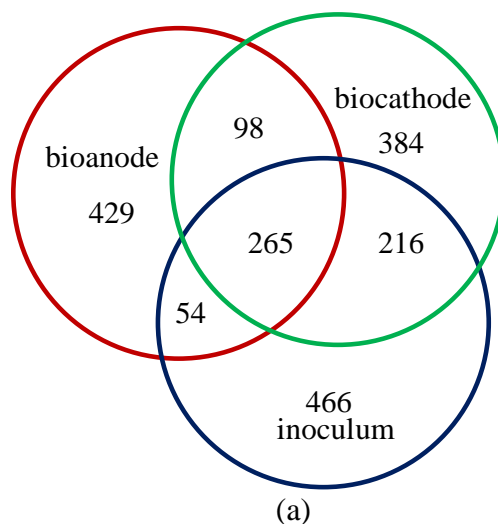


Figure 4. Effect of bioelectrodes for azo dye degradation with abio-electrode as control

Under 0.5 V power supply, the azo dye removal process between the experimental group and control groups could be fitted well by first-order kinetics with the different dynamic response constant (*k*). The *k* of BB group was 0.195 ($R^2 > 99\%$), obviously higher than the BA group of 0.076 ($R^2 > 96\%$), the AB group of 0.009 ($R^2 > 99\%$) and the AA group of 0.003 ($R^2 > 89\%$), respectively.

The result indicated that both EABs could synergistically accelerate the electron transfer between electrode and electron acceptor (or electron donor) and thus improve the azo dye decolorization rate. In BES, the anode EAB is the basis which is mainly responsible for electron generation from substrate. However, the cathode EAB also could determine the final catalytic reaction rate of azo dye if the enough electrons generated from bioanode. Only both EABs formed on electrodes, the BES performance is improved with a better azo dye decolorization effect, comparing to BES without EABs.

3.4 Overall analysis of EAB communities



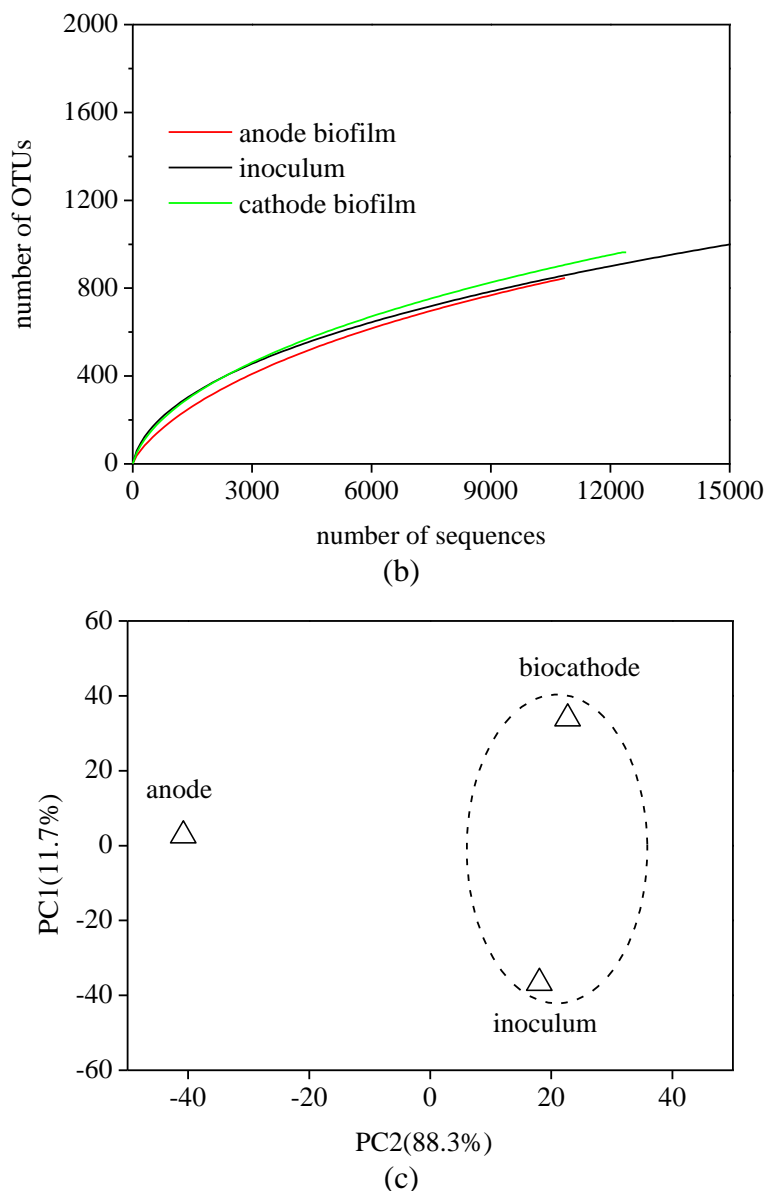


Figure 5. Overall analysis of bacterial communities in anode EAB (bioanode), cathode EAB (biocathode) and initial inoculum (a) Rarefaction curves; (b) Overlap of OTUs; (c) Principal component analysis (PCA)

When the azo dye decolorization test finished, 16s rDNA libraries were analyzed by pyrosequencing from three samples (anode EAB, cathode EAB and inoculum) with 10862, 12301, 15057 reads, respectively. Three libraries contained 846, 963, 1001 operational taxonomic units (OTUs), and shared 265 OTUs with 13.9% of total OTUs (Fig.5A). The rarefaction curves of three samples showed that the OTUs numbers increased slowly when the sequences were more than 10000 reads (Fig.5B). Although the new OTUs are still generated by further pyrosequencing, the coverages have already achieved to 96% at 97% similarity. According to richness and diversity index (Table.1), the inoculum sample had a highest diversity and the anode EAB sample was lowest.

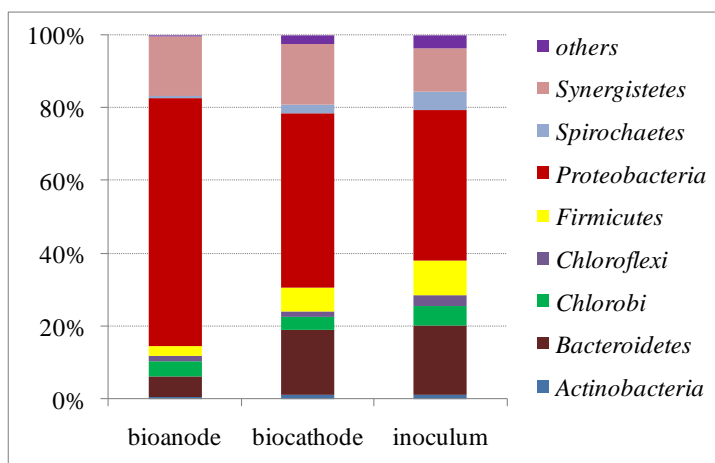
Table 1. Diversity index of bacterial communities in anode EAB, cathodeEAB and inoculum

| Bacterial community | Reads | OTU | ACE index | Chao1 index | Shannon index | Simpson index | coverage |
|---------------------|-------|------|-----------|-------------|---------------|---------------|----------|
| inoculum | 15057 | 1001 | 2360 | 1729 | 4.9 | 0.0229 | 0.97 |
| anode EAB | 10862 | 846 | 1929 | 1432 | 3.76 | 0.0899 | 0.96 |
| cathode EAB | 12301 | 963 | 2253 | 1691 | 4.48 | 0.0475 | 0.96 |

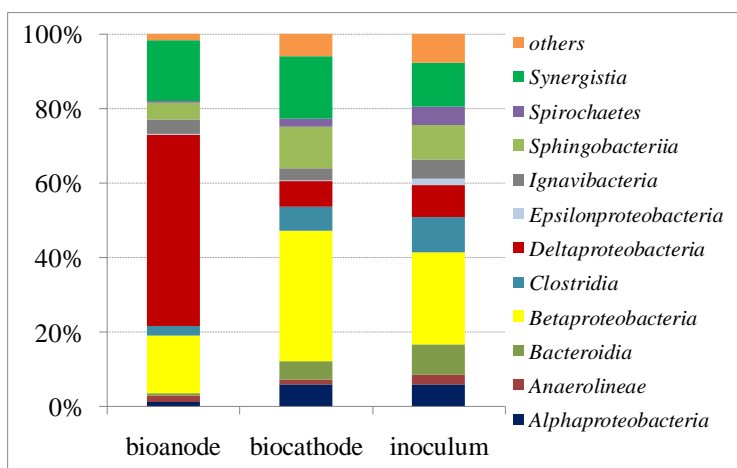
In PCA analysis (Fig.5c), PC1 and PC2 could explain 11.7% and 88.3% of the total community variations, respectively. Three samples were separated from each other, but the cathode EAB had a relative closer relation to inoculum at PC2 level. This PCA result indicated that although both EABs between bioanode and biocathode could be established from the same inoculum, but a distinct difference was on the community structures due to different electrode selectivities. Presumably, the anode EAB revealed a lower microbial diversity that suggested the anode condition is more suitable for exoelectrogens as dominant microbes, considering the the stable ability of electron generation during the azo dye decolorization test. In contrast, cathode EAB was different from anode EAB but a little similar relation with inoculum, suggesting the cathodic condition retains different selectability than anode,.

3.5 Shifts on composition of EAB communities

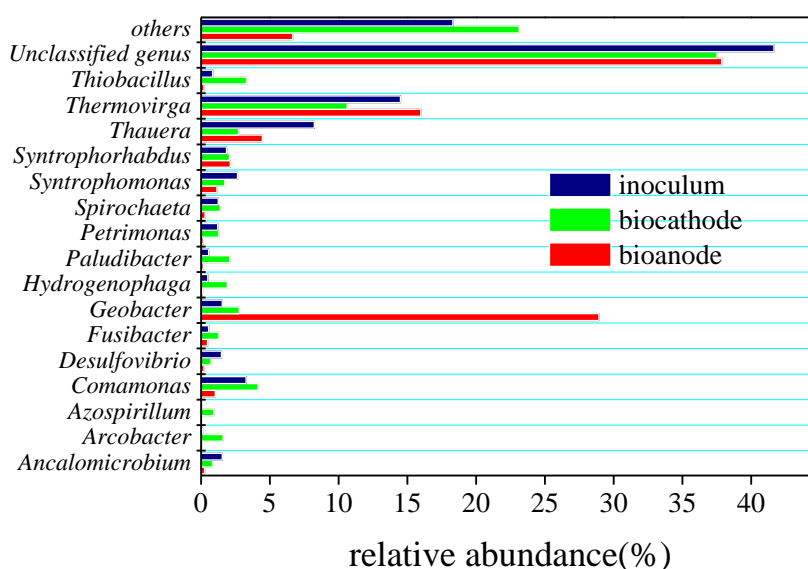
Further analysis of EABs community composition is conducive to validate the above assumption. As seen from Fig.6a, a total of 9 phyla were identified at phylum level. The predominant phylum belonged to *Proteobacteria* (anode EAB 68%, cathode EAB 48%, and inoculums 41%), followed by *Bacteroidetes*, *Synergistetes*. From class level analysis (Fig 6b), anode EAB primarily consisted of *Deltaproteobacteria* (51.3%), *Synergistia* (16.2%), and *Betaproteobacteria* (15.4%). Cathode EAB and inoculum had a similar composition by *Betaproteobacteria* (34.8%, 24.5%), *Synergistia* (16.8%, 11.2%), and *Sphingobacteriia* (11%, 9.1%). An obvious change is *Deltaproteobacteria* which included an important model *Geobacter* with efficient EET function.



(a)



(b)



(c)

Figure 6. Taxonomic classification analysis of bacterial communities in anode EAB(bioanode), cathode EAB(biocathode) and initial inoculum at (a) phylum level; (b) class level; (c) genus level

Further genus level identification (Fig.6c) showed the model electro-active *Geobacter* was dominant in anode EAB (29%), whereas a very low fraction was in the inoculum (1.5%). Although using *Geobacter* usually could reduce electron acceptor, the low abundance in the cathode EAB (2.8%) might suggest that its electrochemical activity still has the potential for further improvement. Not only *Geobacter*, other exoelectrogens were not dominant in the three samples, such as *Shewanella*[21], *Pseudomonas*[22], *Rhodospseudomonas*[23] and *Comamonas*[24]. Following *Geobacter*, *Thermovirga* was subdominant in three samples and researchers did not report its EET function. However, this microbe might contribute to extracellular electron transfer.

For anode EAB, the *Geobacter* is known to have an ability to oxidate the substrate and transfer electrons to anode[25]. As a popular exoelectrogen, *Geobacter* was also found in many other MFC, MEC or other types of BES[26, 27]. For cathode EAB, a high diversity community was found and be different with the anode EAB duo to the different conditions. Comparing to other anaerobic cathode EAB, most of paper used the microbial consortium as inoculum, however, the inoculum usually was

pre-enriched to acclimation. For example, Liang *et al* demonstrated that the cathode EAB can accelerate the reduction of chloramphenicol, using the inoculum from activated sludge acclimated by chloramphenicol[28], as well as Wang *et al* used the nitrobenzene reducing consortium as inoculum to construct the cathode EAB for improving the nitrobenzene degradation. In this paper, we collected the microbial consortium from the effluent as inoculum and did not use the targeted pollutant to acclimate it. It is helpful to evaluate the relation between the electrodes and inoculum.

About EABs formation which enriched from the same inoculum, the effect of inoculum may be not important to anode EAB formation because the anode condition had a high selectivity that benefits to enrich abundant electrochemical active microbes, especially *Geobacter*. The anode EAB proved to be feasible and effective, according to its electrode potential and microbial community composition. However, the microbial community composition of cathode EAB indicated that the cathode condition has the different selectivity comparing to anode. Although the cathode EAB exhibited the efficient capability for azo dye decolorization in this work, the EAB community composition did not find the dominant microbes which about EET or azo dye removal, suggesting that the potentials of cathode EAB need to be further explored for azo dye decolorization. Considering that the cathode EAB was similar with inoculum, improving the inoculum structure should influence the cathode EAB structure. For example, increasing the proportion of functional microbes (electro-active microbes or azo dye degradation microbes) that may be conducive to further enhancing the cathode EAB efficiency.

4. CONCLUSIONS

The aim of this study was to understand the simultaneous EABs formation influenced by the anode and cathode conditions. Based on the same inoculum, both anode EAB and cathode EAB could be established in the single-chamber BES and be effective to azo dye decolorization under different power supply. Anode EAB dominated by a model electro-active *Geobacter* and the cathode EAB microbial structure was relatively similar to the inoculum with low abundance *Geobacter*. In brief, this work provided a suggestion that is improving the inoculum composition would be conducive to play the furthest EAB capability on cathode for recalcitrant pollutant degradation or other applications.

ACKNOWLEDGEMENT

This research was supported by China Postdoctoral Science Foundation (2015M570255), Fundamental Research Funds for the Central Universities of China (N140303002), Postdoctoral Science Foundation of Northeastern University (20150304) and Science Technology Foundation of Liaoning Educational Committee (L20150178).

References

1. H.M. Wang, Z.Y.J. Ren, *Biotechnol Adv*, 31 (2013) 1796-1807.
2. B.E. Logan, B. Hamelers, R. Rozendal, U. Schröder, J. Keller, S. Freguia, P. Aelterman, W. Verstraete, K. Rabaey, *Environ Sci Technol*, 40 (2006) 5181-5192.
3. Y. Du, Y. Feng, Q. Teng, H. Li, *Int. J. Electrochem. Sci*, 10 (2015) 1316-1325.
4. D. Call, B.E. Logan, *Environ Sci Technol*, 42 (2008) 3401-3406.

5. G. Wang, L. Huang, Y. Zhang, *Biotechnol Lett*, 30 (2008) 1959-1966.
6. B. Liang, H.Y. Cheng, D.Y. Kong, S.H. Gao, F. Sun, D. Cui, F.Y. Kong, A.J. Zhou, W.Z. Liu, N.Q. Ren, W.M. Wu, A.J. Wang, D.J. Lee, *Environmental science & technology*, 47 (2013) 5353-5361.
7. Y. Mu, R.A. Rozendal, K. Rabaey, J. Keller, *Environ Sci Technol*, 43 (2009) 8690-8695.
8. A. YI, Y. FENG, Z. DU, H. LI, *Int. J. Electrochem. Sci*, 10 (2015) 1459-1468.
9. Y. Yang, M. Xu, J. Guo, G. Sun, *Process Biochem*, 47 (2012) 1707-1714.
10. D.R. Lovley, *Annual Review Of Microbiology*, Vol 66, 66 (2012) 391-409.
11. B. Virdis, S.T. Read, K. Rabaey, R.A. Rozendal, Z. Yuan, J. Keller, *Bioresource Technol*, 102 (2011) 334-341.
12. A.J. Wang, H.Y. Cheng, B. Liang, N.Q. Ren, D. Cui, N. Lin, B.H. Kim, K. Rabaey, *Environmental science & technology*, 45 (2011) 10186-10193.
13. K.P. Nevin, T.L. Woodard, A.E. Franks, Z.M. Summers, D.R. Lovley, *Mbio*, 1 (2010).
14. A.P. Borole, G. Reguera, B. Ringeisen, Z.W. Wang, Y.J. Feng, B.H. Kim, *Energy & Environmental Science*, 4 (2011) 4813-4834.
15. B. Erable, I. Vandecandelaere, M. Faimali, M.-L. Delia, L. Etcheverry, P. Vandamme, A. Bergel, *Bioelectrochemistry*, 78 (2010) 51-56.
16. Y. Yang, Y. Xiang, G. Sun, W.-M. Wu, M. Xu, *Environ Sci Technol*, (2014).
17. Y.Z. Wang, A.J. Wang, W.Z. Liu, Q. Sun, *Bioresource Technol*, 142 (2013) 688-692.
18. A. Zhou, W. Liu, C. Varrone, Y. Wang, A. Wang, X. Yue, *Bioresource Technol*, 192 (2015) 835-840.
19. Y.Z. Wang, A.J. Wang, W.Z. Liu, D.Y. Kong, W.B. Tan, C. Liu, *Bioresource Technol*, 146 (2013) 740-743.
20. Q. Sun, Z.L. Li, W.Z. Liu, D. Cui, Y.Z. Wang, J.S. Chung, A.J. Wang, *International Journal of Electrochemical Science*, 11 (2016) 2447-2460.
21. B.R. Ringeisen, E. Henderson, P.K. Wu, J. Pietron, R. Ray, B. Little, J.C. Biffinger, J.M. Jones-Meehan, *Environ Sci Technol*, 40 (2006) 2629-2634.
22. N. Boon, K. De Maeyer, M. Höfte, K. Rabaey, W. Verstraete, *Appl Microbiol Biot*, 80 (2008) 985-993.
23. D. Xing, Y. Zuo, S. Cheng, J.M. Regan, B.E. Logan, *Environ Sci Technol*, 42 (2008) 4146-4151.
24. D. Xing, S. Cheng, B.E. Logan, J.M. Regan, *Appl Microbiol Biot*, 85 (2010) 1575-1587.
25. K.P. Nevin, B.C. Kim, R.H. Glaven, J.P. Johnson, T.L. Woodard, B.A. Methe, R.J. DiDonato, S.F. Covalla, A.E. Franks, A. Liu, D.R. Lovley, *Plos One*, 4 (2009).
26. L. Lu, D.F. Xing, N.Q. Ren, B.E. Logan, *Bioresource Technol*, 124 (2012) 68-76.
27. U. Michaelidou, A. ter Heijne, G.J.W. Euverink, H.V. Hamelers, A.J. Stams, J.S. Geelhoed, *Appl Environ Microb*, 77 (2011) 1069-1075.
28. B. Liang, H.Y. Cheng, D.Y. Kong, S.H. Gao, F. Sun, D. Cui, F.Y. Kong, A.J. Zhou, W.Z. Liu, N.Q. Ren, *Environ Sci Technol*, 47 (2013) 5353-5361.